International Journal of Thermophysics, Vol. 8, No. 1, 1987

The Thermal Conductivity Surface for Mixtures of Methane and Ethane

D. G. Friend[1] and H. M. Roder[1]

Received February 24, 1986

A correlation is presented for the extensive series of thermal conductivity measurements of binary methane–ethane mixtures. The composition dependences of the thermal conductivity in the dilute-gas region, dense-gas and liquid region, and critical region are discussed. The average absolute percentage deviation of the thermal conductivity surface as a function of temperature, density, and composition, from the experimental data, is 1.60%.

KEY WORDS: correlation; ethane; methane; mixtures; thermal conductivity.

1. INTRODUCTION

The recent extensive measurements of the thermal conductivity of methane, ethane, and three of their binary mixtures enable us to examine the structure of the thermal conductivity surface over a broad range of temperature, density, and composition for the methane–ethane fluid system. In this paper, we present a simple correlation which represents the nearly 4200 data points to within less than 2% average absolute deviation (or 3 $mW \cdot m^{-1} \cdot K^{-1}$ RMS deviation). In addition, we discuss the composition dependences of the three contributions to the thermal conductivity, namely, the dilute gas, the excess term, and the critical enhancement. Comparison with certain other predictive correlations is also made.

In previous publications we have described the apparatus [1], presented both data and correlations for pure methane [2] and ethane [3], and discussed the data and correlations for fixed compositions of the three binary mixtures [4]. Thus, our present emphasis is on a global correlation and the composition dependences. In Section 2 we present an overview of

[1] Thermophysics Division, National Bureau of Standards, Boulder, Colorado 80303, U.S.A.

0195-928X/87/0100-0013$05.00/0

the data and the previously developed correlations; next we examine the dilute gas thermal conductivity as a function of composition; and in Sections 4 and 5 we deal with the excess term and the critical enhancement, respectively. Section 6 gives the global correlation, and finally, Section 7 summarizes our results.

2. DATA AND CONSTANT-COMPOSITION CORRELATIONS

The data consist of 4173 points for five samples with methane mole fractions 1.0, 0.685, 0.502, 0.345, and 0.0 (denoted henceforth as CH_4,

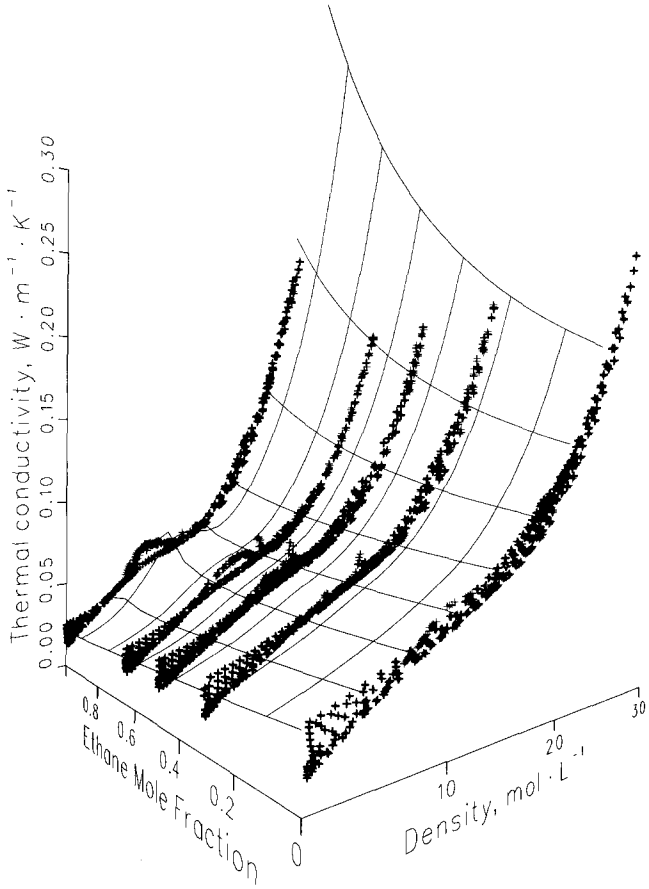

Fig. 1. Experimental thermal conductivity for all measured temperatures, densities, and (ethane) mole fractions. The lines represent 300 K isotherms calculated from the global correlation of Eq. (7) at fixed density or fixed composition.

70/30, 50/50, 35/65, and C_2H_6, respectively) at temperatures between 140 and 330 K and densities to 30 mol · L^{-1} measured in this laboratory. Additional data for pure ethane at higher temperatures, measured by Prasad and Venart [5], have also been used to develop the global correlation but were not used in the final determination of the coefficients. In Fig. 1, we present all of our data.

For each of the samples, we have developed [4] a constant-composition correlation of the form

$$\begin{aligned}\lambda(\rho, T) &= \lambda_0(T) + \lambda_{ex}(\rho, T) + \Delta\lambda_c(\rho, T) \\ &= A_1 + A_2 T + A_3 T^2 + (B_1 + B_2 T)\rho + (B_3 + B_4 T)\rho^3 + B_5\rho^5 \\ &\quad + \left[\frac{C_1}{T_0 + C_2} + C_3 + C_4 T_0\right] \exp\{-[C_0(\rho - \rho_{cen})]^2\}\end{aligned} \tag{1}$$

with

$$T_0 = T\eta(T - T_c) + T_c\eta(T_c - T) \tag{1a}$$

and

$$C_0 = C_6\eta(\rho - \rho_{cen}) + C_5\eta(\rho_{cen} - \rho) \tag{1b}$$

In Eqs. (1), (1a), and (1b), T and ρ are the temperature (in K) and density (in mol · L^{-1}), respectively. The A's, B's, and C's are composition-dependent parameters (with A's associated with λ_0, B's with λ_{ex}, and C's with $\Delta\lambda_c$); T_c is the (x-dependent) critical temperature; ρ_{cen} is the (x-dependent) centering density which is close to the critical density. The step function, η, is defined to be +1 when the argument is positive; otherwise it is zero. The parameters and a measure of the goodness of fit (average absolute percentage error, DEVS) for each of the five compositions are given in Table I. We note that 80 parameters are needed and mention that, in general, the constants are not linear functions of composition. Except for pure methane and ethane, the parameters for Eq. (1) have been presented previously [4].

3. DILUTE-GAS THERMAL CONDUCTIVITY

The dilute-gas thermal conductivity, λ_0, can be obtained from the present data by extrapolation to zero density. At very low temperatures the saturation boundaries for the pure components and the dew points of the mixtures occur at low pressures, and data along an isotherm are sparse. For these temperatures, the correlations in Section 2 were used to aid the extrapolation. Values for λ_0, adjusted by the correlation of Eq. (1) to nominal temperatures, are plotted in Fig. 2.

Table I. Parameters for Fixed-Composition Correlations [Eq. (1)]

	CH_4	70/30	50/50	35/65	C_2H_6
A_1	0.1892461E−02	0.1876327E−02	0.9271600E−02	0.2849547E−01	0.1804961E−01
A_2	0.7443056E−04	0.3060668E−04	−0.3606085E−04	−0.1971104E−03	−0.1184817E−03
A_3	0.1041690E−06	0.1941864E−06	0.3047760E−06	0.6064916E−06	0.4243877E−06
B_1	0.2415794E−02	0.2091574E−02	0.2281903E−02	0.2294100E−02	0.3170513E−02
B_2	−0.9168256E−06	0.6109347E−06	0.1157403E−06	−0.1757653E−05	−0.2373898E−05
B_3	0.2415394E−05	0.5868615E−05	0.4184580E−05	0.1023516E−04	0.7848724E−05
B_4	0.5916165E−08	0.3105442E−08	0.9001806E−08	0.8856678E−08	0.1743757E−07
B_5	0.4560196E−08	0.5910959E−08	0.1243893E−07	0.6095560E−08	0.2115329E−07
C_1	0.3597701E+00	0.2766677E+00	0.2953032E+00	0.6371161E−01	0.6230209E−03
C_2	−0.1805550E+03	−0.2240000E+03	−0.2425000E+03	−0.2729000E+03	−0.2953300E+03
C_3	−0.2753952E−02	0.1827450E−01	0.3256997E−01	0.6649022E−01	0.2560443E+00
C_4	0.8971779E−05	−0.5571235E−04	−0.9394503E−04	−0.1753457E−03	−0.7410801E−03
C_5	−0.2242437E+00	−0.2212507E+00	−0.2243679E+00	−0.2242510E+00	−0.3181729E+00
C_6	0.1780728E+00	0.2119179E+00	0.2357194E+00	0.2417181E+00	0.3176916E+00
T_c	0.1905550E+03	0.2397790E+03	0.2629190E+03	0.2789100E+03	0.3053300E+03
ρ_{cen}	0.1000000E+02	0.8750000E+01	0.8680000E+01	0.8060000E+01	0.6800000E+01
DEVS (%)	0.61	0.87	1.14	1.09	1.22

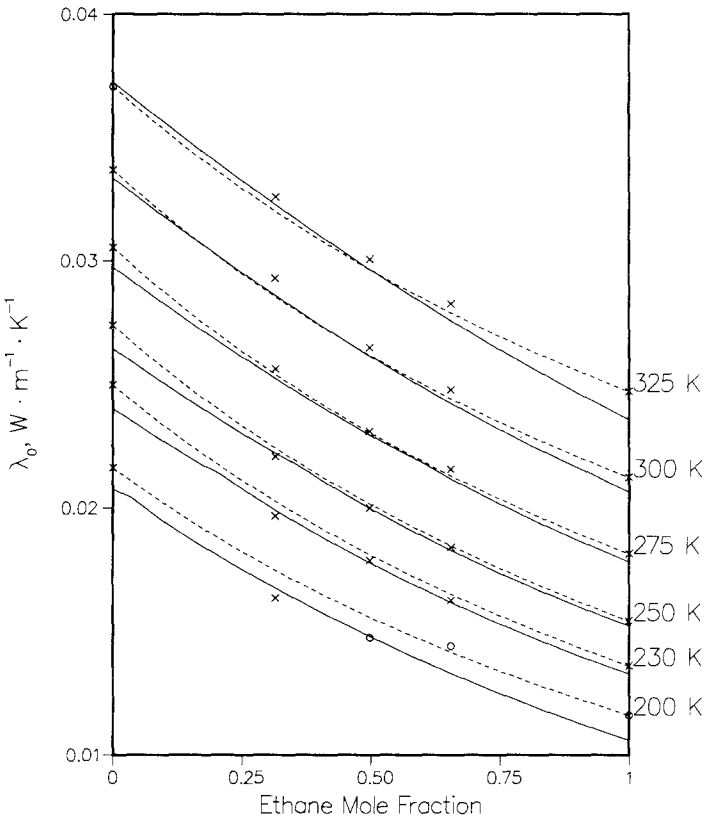

Fig. 2. Dilute-gas thermal conductivity. The points (x) represent extrapolations of experimental data adjusted to nominal temperatures by Eq. (1). Open circles fall outside the range of the data. Solid lines represent the global fit of Eq. (7). Dashed lines represent the Chapman–Enskog mixture theory (forced to agree with the data for the pure components).

The constant-composition correlations in Eq. (1) involve three terms for the dilute-gas thermal conductivity and consist of a constant and terms linear and quadratic in temperature. The present global correlation uses terms proportional to $T^{\frac{1}{2}}$ to minimize the composition dependence of the temperature coefficients. The precise form of this correlation is given below in Eq. (7) and the dilute-gas values obtained from this correlation are illustrated in Fig. 2 as solid lines. The anomalous bumps in Fig. 2 occur because the critical enhancement of Section 5 cannot be forced to be zero at low density when the temperature is near the critical temperature of a mixture.

The rigorous dilute-gas transport coefficient results of the Chapman–Enskog [6] theory become less tenable when applied to mixtures of polyatomic gases. In Fig. 2 the curves shown are based on Lennard–Jones (12-6) collision integrals [7] with the well depth and zero crossing (ε and σ) determined from viscosity data for the pure components [8] and calculated as the geometric mean (ε) and arithmetic mean (σ) for the interspecies potential parameters. The experimental Eucken factors are used for the pure methane and ethane (forcing the curves to the correct values at $x = 0$ and $x = 1$). For mixtures, these factors and the theoretically calculated diffusion coefficients contribute to the mixture thermal conductivity as in the Chapman–Cowling first-order formula used by Clifford et al. [9]. Attempts made to calculate the Eucken factors for pure methane and ethane using known specific heat values with either the original or the modified Eucken correlation were less than satisfactory. Analysis of the dilute-gas conductivity using the Mason–Monchick theory [10] or other approximations for the pure components was not attempted.

An experimental correlation developed by Bolotin et al. [11] (and not illustrated) gives good agreement for ethane-rich mixtures but deteriorates to about the 10% level as the methane mole fraction increases. The TRAPP (1981) [12] correlation (not illustrated), which is optimized as a global correlation for many different fluids and their multicomponent mixtures, does not adequately describe this system at low density. While the shapes of the TRAPP isotherms conform well to the present data, the dilute-gas values are in error by up to nearly 10%. This is equivalent to a systematic error of 25 K but is essentially within the stated uncertainty of Ref. 12.

4. EXCESS THERMAL CONDUCTIVITY

The excess thermal conductivity is conventionally defined as the difference

$$\lambda_{ex}(\rho, T, x) = \lambda(\rho, T, x) - \lambda_0(T, x) - \Delta\lambda_c(\rho, T, x) \tag{2}$$

where λ is the total conductivity, λ_0 was discussed in the previous section, and $\Delta\lambda_c$ is the critical enhancement discussed in Section 5. In this section and the associated Fig. 3 we have used the fixed-composition fits of λ_0 and $\Delta\lambda_c$ to evaluate λ_{ex}.

The initial density dependence of transport properties (i.e., the first term in a density expansion of λ_{ex}) has been a subject of considerable theoretical interest. However, the recent rigorous theoretical developments [13] have not been extended to mixtures of polyatomic molecules.

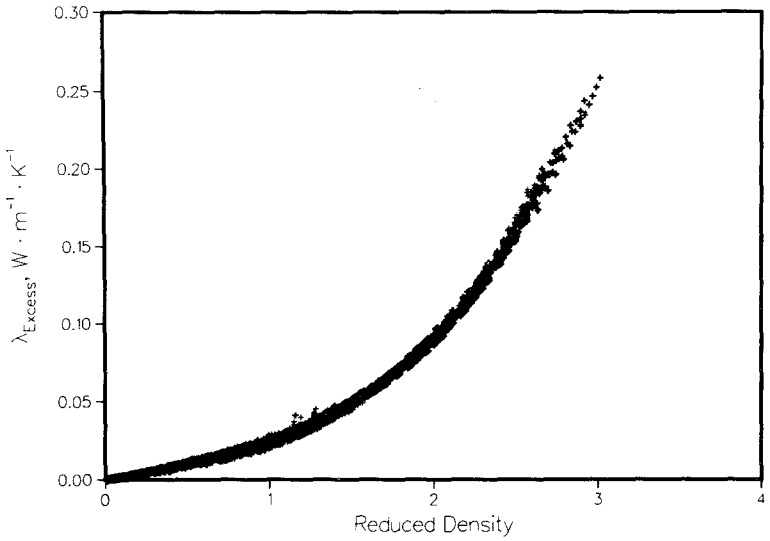

Fig. 3. Experimental excess thermal conductivity (all points) versus reduced density.

Additionally, the logarithmic terms theoretically predicted [14] for isothermal density expansions are not particularly significant when developing correlations with experimental data. Thus, for the correlations of constant composition, the density expansion uses the first three odd powers of density with temperature dependences in the linear and cubic terms. In fact, the temperature dependence of λ_{ex} is very small, but it can be seen in deviation plots at high density, where different isotherms show slightly different behavior.

To achieve a global correlation of the excess conductivity, it is useful to consider a reduced density as the independent variable. If one uses the critical densities of each of the five systems as the reduction parameters, the spread of the conductivity versus reduced density curve is substantially decreased. If a linear approximation to the critical density is used, i.e.,

$$\rho_c(x) = \rho_c^{CH_4} + x(\rho_c^{C_2H_6} - \rho_c^{CH_4})$$

where the pure-fluid critical densities are exactly retained, the three mixtures conform well to the methane excess thermal conductivity; however, the ethane curve remains separate, presumably due to the shape of the ethane molecule. To achieve universality for the five systems, a linear model for the reduction parameter $\rho_c(x)$ was used, with the slope con-

Table II. Constants, Nonlinear Parameters, and Coefficients Used in Eq. (7)

Constants					
$\rho_c^{CH_4}$	$T_c^{CH_4}$	$T_c^{C_2H_6}$	M_1	M_2	
$10.0\ \text{mol} \cdot \text{L}^{-1}$	190.555 K	305.33 K	16.043	30.070	
Nonlinear parameters					
β_ρ	τ	ψ	σ_1	σ_2	
$-2.794\ \text{mol} \cdot \text{L}^{-1}$	0.56	0.525	$3.42\ \text{mol} \cdot \text{L}^{-1}$	$-1.28\ \text{mol} \cdot \text{L}^{-1}$	
Coefficients					
α_1	α_2	α_3	α_4	α_5	α_6
0.9827×10^{-3}	-0.9387×10^{-3}	0.7843×10^{-6}	0.2174×10^{-5}	0.7846×10^{-8}	-0.5009×10^{-8}
β_1	β_2	β_3			
0.2362×10^{-1}	0.3736×10^{-2}	0.4138×10^{-3}			
γ_1	γ_2	γ_3			
0.3328×10^{-2}	-0.5028×10^{-2}	-0.6550×10^{-2}			

sidered an adjustable parameter. For the global fit, then, the density reduction used in the excess conductivity satisfied

$$\begin{aligned}\rho_c(x) &= \rho_c^{CH_4} + x(\rho_r - \rho_c^{CH_4}) \\ &= \rho_c^{CH_4} + \beta_\rho x\end{aligned} \tag{3}$$

where $\rho_r = 7.206\ \text{mol} \cdot \text{L}^{-1}$ (which differs from $\rho_c^{C_2H_6}$ by 6%). Note that $\rho_c(x)$ defined by Eq. (3) differs slightly from the mixture critical density and the enhancement centering density (except for pure methane).

In Fig. 3, we plot λ_{ex} versus reduced density [defined by $\rho_x^* = \rho/\rho_c(x)$] for the five systems. A polynomial fit in ρ_x^*, analogous to the excess correlation at fixed composition, was used to approximate the universal curve. Thus we use

$$\lambda_{ex}(\rho, T, x) = \beta_1 \rho_x^* + \beta_2(\rho_x^*)^3 + \beta_3(\rho_x^*)^5 \tag{4}$$

where the values of the β's are given in Table II.

5. CRITICAL ENHANCEMENT

The behavior of the thermal conductivity in the region of mixture critical points has been the subject of recent interest [15, 16], including a paper by the present authors [17] discussing the methane–ethane data. The experimental enhancement data as well as constant-composition fits are displayed in Fig. 4 of Ref. 2 for methane, Fig. 3 of Ref. 3 for ethane, and Fig. 3 of Ref. 4 for the mixtures. In this section, then, we concentrate on the x dependence of the critical anomaly in order to complete our global correlation.

From Eq. (1) we note that the fixed-composition correlations approximate the density dependence of the critical enhancement by a Gaussian function which is slightly asymmetric about the (x-dependent) centering density. Other authors use a Lorentzian lineshape for the density dependence [18]. This centering density is quite close to the critical density and seems to be temperature independent. The asymmetry $[(|C_5| - |C_6|)/|C_5|$ in Eq. (1)] ranges from 0.15% for ethane to 20.6% for methane and we choose to ignore it for simplicity of the global fit. The temperature-independent widths, $\Delta\rho$, of the enhancement curves [i.e., full width at half-maximum, $2\sqrt{\ln 2}/C_0$, where C_0 is defined in Eq. (1b)] range from about $5.2\ \text{mol} \cdot \text{L}^{-1}$ for $\rho < \rho_{cen}$ in ethane to $9.4\ \text{mol} \cdot \text{L}^{-1}$ for $\rho > \rho_{cen}$ in methane as shown in Fig. 4. A linear approximation, $\Delta\rho = 8.04 - 3.01x$, was chosen to give the best overall fit to

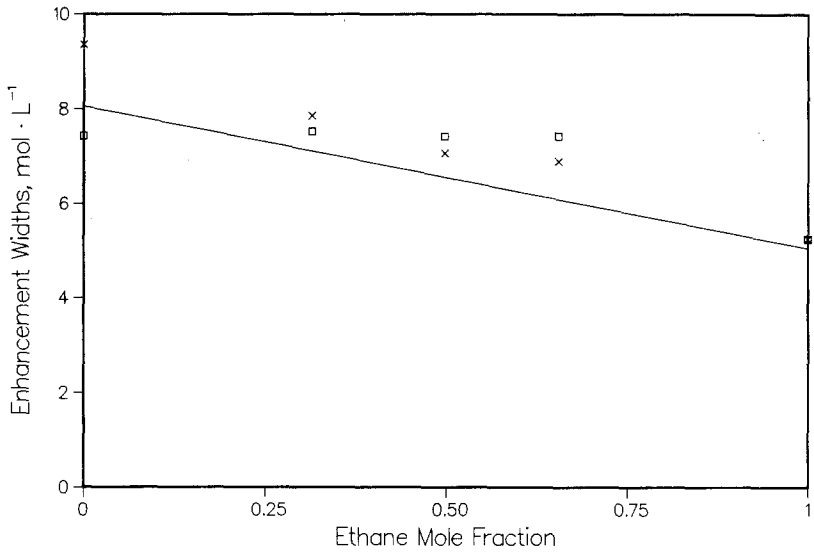

Fig. 4. Density width of the critical enhancement versus mole fraction. Points are from fits of Eq. (1), with symbol x when $\rho > \rho_{cen}$ and □ when $\rho < \rho_{cen}$. Solid line represents approximation used in global fit.

the data and is also illustrated in Fig. 4. This corresponds to an expression for the standard deviation in the Gaussian function, of the form

$$\sigma_x = \sqrt{\frac{2}{\ln 2}} \frac{\Delta\rho}{4} = \sigma_1 + \sigma_2 x \qquad (5)$$
$$= 3.42 - 1.28x$$

To evaluate the temperature dependence of the critical enhancement along the critical isochore (or more precisely, the centering isochore), we note that, when plotted against reduced temperature $[\Delta T^* = (T - T_c)/T_c]$, the five systems are qualitatively similar. This is seen in Fig. 5 of Ref. 4, which uses experimental values of the amplitudes, $\Delta\lambda_{c(x)}(\rho_{cen}, \Delta T^*)$. Because of the shapes of the two-phase region for mixtures and the large differences among the critical temperatures, experimental values of $\Delta\lambda_c(\rho_{cen}, \Delta T^*)$ versus x at constant reduced temperatures are not readily available. Hence, in Fig. 5, we illustrate the concentration dependence of the amplitudes at constant reduced temperatures using the Eq. (1) fits to $\Delta\lambda_c(\rho_{cen}, \Delta T^*)$ for the mixtures and a fit of Fig. 5 in Ref. 4 for the pure methane and ethane. The value of $\Delta\lambda_c(\rho_{cen})$ can be strongly dependent on the background conductivity used.

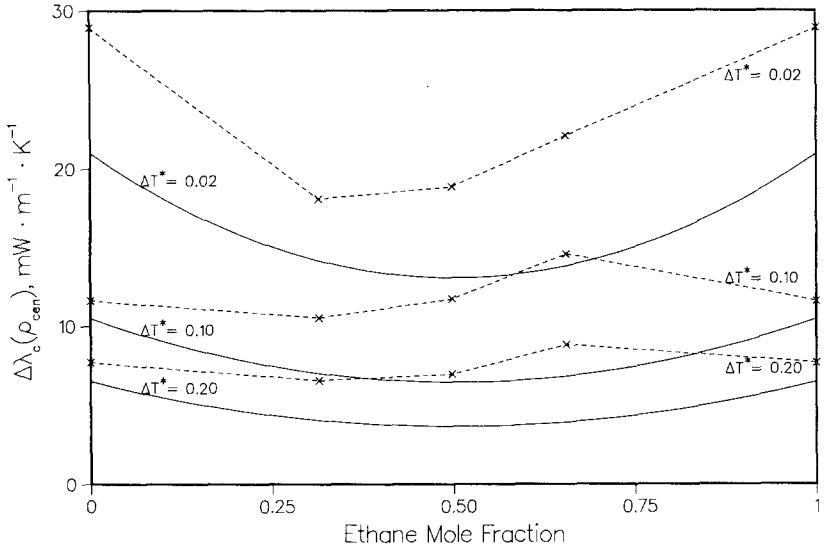

Fig. 5. Amplitude of the critical enhancement versus the mole fraction. The "experimental" points (x) are from a fit of the "universal" enhancement curve (i.e., Fig. 5 of Ref. 4) for the pures and from Eq. (1) for the mixtures. Points of constant reduced temperature are connected by dashed lines to guide the eye. The solid lines represent the fit of Eq. (7).

The composition dependence of the amplitude seems highly irregular and is not smoothed by focusing on a reduced amplitude [$\Delta\lambda^* = \Delta\lambda/(\lambda_0 + \lambda_{ex})$]. There may be a hint of the crossover phenomenon to non-divergent behavior for the mixtures. However, the curves, with shape not definitely established by the current data, seem not to drop as sharply as is calculated by one-fluid corresponding-states models [19]. Rather than attempt a theoretically based correlation requiring additional thermodynamic and transport data, we have chosen to establish the composition and temperature dependences of the amplitude empirically.

The critical temperatures used to compute ΔT^* can be modeled as a linear mass fraction average [20],

$$T_c(x) = T_c^{CH_4} + \frac{xM_2}{(1-x)M_1 + xM_2}(T_c^{C_2H_6} - T_c^{CH_4}) \tag{6a}$$

where M_1 and M_2 are the methane and ethane molar masses, respectively. Deviations from the actual critical temperatures are less than 4 K or 1.6% for the systems used. The amplitude near the critical temperature behaves

like a power-law singularity in ΔT^* and drops to zero faster than the power law would imply. Thus we approximate the amplitude as

$$\Delta\lambda_c[\rho_c(x), T, x] = [\gamma_1 + \gamma_2 x(1-x) + \gamma_3 e^{-\tau/[|\Delta T^*| + 0.01]}] \cdot [|\Delta T^*| + 0.01]^{-\psi} \tag{6b}$$

The critical exponent ψ is found from the global fit to be 0.525, whereas Cohen et al. [16] found an exponent of 0.58 for the ^{3}He–^{4}He system. The coefficients γ_1, γ_2, and γ_3 and the parameter τ that give the best global fit are given in Table II. The numerical value of 0.01 in Eq. (6) is simply to prevent singularities in the correlation. The amplitudes derived from Eq. (6) are shown in Fig. 5.

6. GLOBAL CORRELATION

The discussion of λ_0, λ_{ex}, and $\Delta\lambda_c$ produces a global correlation of the form

$$\begin{aligned}\lambda(\rho, T, x) &= \lambda_0(T, x) + \lambda_{ex}(\rho, T, x) + \Delta\lambda_c(\rho, T, x) \\ &= T^{\frac{1}{2}}[\alpha_1 + \alpha_2 x + (\alpha_3 + \alpha_4 x^2)T + (\alpha_5 + \alpha_6 x^2)\, T^2] \\ &\quad + \beta_1 \rho_x^* + \beta_2 \rho_x^{*3} + \beta_3 \rho_x^{*5} \\ &\quad + \{\gamma_1 + \gamma_2 x(1-x) + \gamma_3 e^{-\tau/[|\Delta T_x^*| + 0.01]}\} \\ &\quad \cdot [|\Delta T_x^*| + 0.01]^{-\psi}\, e^{-\frac{1}{2}[(\rho - \rho_c(x))/\sigma_x]^2}\end{aligned} \tag{7}$$

where ρ, T, and x are, respectively, the density in mol $\cdot$ L^{-1}, the temperature in K, and the ethane mole fraction. The reduced density is defined by $\rho_x^* = \rho/\rho_c(x)$, where $\rho_c(x)$ is defined in Eq. (3). The reduced temperature is defined by $\Delta T^* = [T - T_c(x)]/T_c(x)$, with $T_c(x)$ defined by Eq. (6a). Finally, the width σ_x of the Gaussian density function is given by Eq. (5).

In the global correlation, we used five constants ($\rho_c^{CH_4}$, $T_c^{CH_4}$, $T_c^{C_2H_6}$, M_1, and M_2), 12 coefficients which were fit using linear regression ($\alpha_{1\text{-}6}$, $\beta_{1\text{-}3}$, $\gamma_{1\text{-}3}$), and five parameters fit by nonlinear techniques (β_ρ, τ, ψ, σ_1, and σ_2). Values of all these are given in Table II.

The global average absolute percentage deviation of the experimental points from the correlation of Eq. (7) was 1.60% (or rms deviation 2.55 mW $\cdot$ m^{-1} $\cdot$ K^{-1}). For the five individual systems, in order of increasing ethane mole fractions, the average absolute percentage deviations were 1.02, 1.48, 1.73, 1.61, and 2.24%. Deviation plots for all measured points are given in Fig. 6. Much of the error comes from the high-density liquid points as well as in the critical region (especially for ethane).

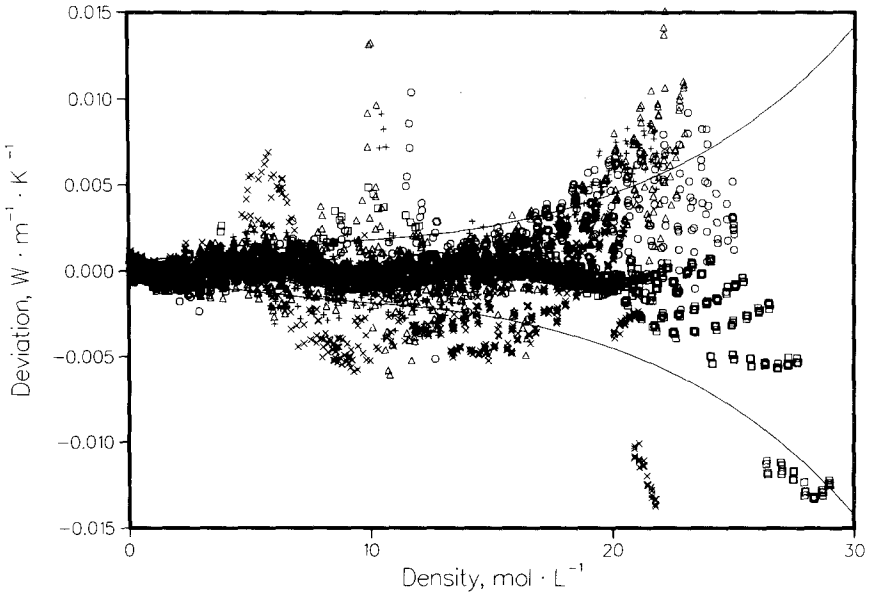

Fig. 6. Deviation of experimental points from the correlation of Eq. (7). The symbols represent experimental points as follows: □, CH_4; ○, 70/30; △, 50/50; +, 35/65; ×, C_2H_6. The solid lines represent deviations of ±3% for a mixture with $X = 0.50$ at $T = 250$ K.

7. CONCLUSION

The measurement of nearly 4200 thermal conductivity data points over a large range of temperature, density, and composition gives us a unique opportunity to examine the behavior of the thermal conductivity surface for a binary mixture. We first emphasize that the qualitative behavior of the thermal conductivity, including the presence of an enhancement near the critical point, is independent of composition. Perhaps closer study of the critical point would alter this conclusion and give stronger evidence for a crossover to nonanomalous behavior.

The empirical correlation of Eq. (7) represents an excellent fit to the large data set and, we believe, is a good representation of the thermal conductivity surface for all compositions of the binary methane–ethane system within a temperature range of 140–330 K with densities up to about 24 mol · L^{-1}. This correlation gives a better description of the methane–ethane data than the predictive correlation of TRAPP [12], especially in the low-density and nearly critical regions. The application of this form of correlation to other binary mixtures has not been attempted.

ACKNOWLEDGMENT

Partial support from the Gas Research Institute is gratefully acknowledged.

REFERENCES

1. H. M. Roder, *J. Res. Natl. Bur. Stand. (U.S.)* **86**:457 (1981).
2. H. M. Roder, *Int. J. Thermophys.* **6**:119 (1985); Experimental Thermal Conductivity Values for Hydrogen, Methane, Ethane and Propane, Natl. Bur. Stand. (U.S.) Interagency Report NBSIR 84-3006 (1984).
3. H. M. Roder and C. A. Nieto de Castro, *High Temp. High Press.* **17**:453 (1985).
4. H. M. Roder and D. G. Friend, *Int. J. Thermophys.* **6**:607 (1985); Experimental Thermal Conductivity Values for Mixtures of Methane and Ethane, Natl. Bur. Stand. (U.S.) Interagency Report NBSIR 85-3024 (1985).
5. R. C. Prasad and J. E. S. Venart, *Int. J. Thermophys.* **5**:367 (1984).
6. J. O. Hirschfelder, C. F. Curtiss, and R. B. Bird, *Molecular Theory of Gases and Liquids* (John Wiley, New York, 1954), Chaps. 7 and 8.
7. P. D. Neufeld, A. R. Janzen, and R. A. Aziz, *J. Chem. Phys.* **57**:1100 (1972).
8. R. C. Reid, J. M. Prausnitz, and T. K. Sherwood, *The Properties of Gases and Liquids* (McGraw–Hill, New York, 1977).
9. A. A. Clifford, R. D. Fleeter, J. Kestin, and W. A. Wakeham, *Ber. Bunsenges. Phys. Chem.* **84**:18 (1980).
10. E. A. Mason and L. Monchick, *J. Chem. Phys.* **36**:1622 (1962).
11. N. K. Bolotin, E. K. Dregulyas, A. Y. Kolomiets, V. P. Provator, and A. M. Shelomentsev, Teplofiz. Svoistva Gazov. (Mater. Vses. Teplofiz. Svoistvam) (5th, Kiev, 1974) (1976), pp. 90–97.
12. J. F. Ely and H. J. M. Hanley, A Computer Program for the Prediction of Viscosity and Thermal Conductivity in Hydrocarbon Mixtures, Natl. Bur. Stand. (U.S.) Technical Note 1039 (1981).
13. D. G. Friend and J. C. Rainwater, *Chem. Phys. Lett.* **107**:590 (1984).
14. A. Gervois and Y. Pomeau, *Phys. Rev.* **A9**:2196 (1974).
15. L. Mistura, *Nuovo Cim.* **12B**:35 (1972); A. Onuki, *J. Low Temp. Phys.* **61**:101 (1985).
16. L. H. Cohen, M. L. Dingus, and H. Meyer, *J. Low Temp. Phys.* **49**:545 (1982); *Phys. Rev. Lett.* **50**:1058 (1983); *J. Low Temp. Phys.* **61**:79 (1985).
17. D. G. Friend and H. M. Roder, *Phys. Rev.* **A32**:1941 (1985).
18. B. Le Neindre, Y. Garrabos, and R. Tufeu, *Ber. Bunsenges. Phys. Chem.* **88**:916 (1984).
19. H. J. M. Hanley, *J. Res. Natl. Bur. Stand. (U.S.)* **82**:181 (1977).
20. O. T. Bloomer, D. C. Gami, and J. D. Parent, Physical-Chemical Properties of Methane-Ethane Mixtures, IGT Bulletin 22 (July 1953).